Supplementary Methods

"Differences in prion strain conformations result from nonnative interactions in a nucleus"

Yumiko Ohhashi, Kazuki Ito, Brandon H. Toyama, Jonathan S. Weissman &
Motomasa Tanaka

Supplementary Methods

***In vitro* analysis of Sup35NM monomer and oligomer.** CD spectra of soluble Sup35NM (3-15μM) in 5mM potassium phosphate buffer including 150mM sodium chloride were measured with a J-720 spectrophotometer (JASCO) equipped with a peltier thermal controller, a scan speed of 10nm/min, and a resolution of 0.2nm. For Sup35NM amyloid, the amyloid solution in 5mM potassium phosphate buffer including 150mM sodium chloride was sonicated for 10sec with a Branson sonifier (20%).

Velocity AUC experiments were performed in a Beckman Optima XL-I analytical ultracentrifuge using an An60Ti rotor at 4 or 37°C. Data were analyzed with Sedfit using c(S) distribution method (http://www.analyticalultracentrifugation.com)[1]. The parameters for calculating the number of Sup35NM monomers in an oligomer are as follows: density, 1.00693; viscosity, 1.5913e-2; partial specific volume, 0.73; frictional ratio, 2.263260; rmsd, 0.032371.

The measurement of SAXS was performed at the SAXS-dedicated beamline BL45XU[2,3] in SPring-8, operated by RIKEN, Japan. The sample-to-detector distance was 2.2m and the wavelength used was 0.9Å. The temperature of the sample (typically 18μM) was controlled by a high-precision peltier thermal controller (±0.05°C). Using an X-ray image intensifier and cooled CCD detector (XR-II+CCD)[4], each scattering image was collected for 1sec during which no radiation damage was found. The scattering image was converted into 1D profile and corrected for the contrast reduction[5]. The 1D profiles were normalized to the intensity of the incident beam monitored by ionization chamber in front of the sample and the profile of buffer alone was subtracted. The radius of gyration (R_g) was determined by the Guinier approximation: $I(S)\sim I(0)\exp(-4\pi^2 R g^2 S^2/3)$, where S and $I(0)$ are the momentum transfer and intensity at the zero scattering angle, respectively. S is defined as $S=2\sin\theta/\lambda$, where 2θ and λ are the

scattering angle and the X-ray wavelength, respectively[6]. The range $S<0.002$ corresponds to an inaccessible region including parasitic scattering. The Kratsky plot was calculated as previously reported[7].

Fluorescence of thioflavine T was measured with a fluorescence spectrophotometer (FL-7000, Hitachi) equipped with a thermal controller of water bath. Excitation of thioflavine T fluorescence was 442nm and emission was monitored at 485nm. Concentration of thioflavine T was 20μM and Sup35NM concentration varied from 5μM to 15μM.

Introduction of *in vitro* Sup35NM amyloid into yeast and determination of prion strain phenotypes. Yeast spheroplasts of the [*psi*$^-$][*PIN*$^+$] 74D-694 strain [MATa, *his3*, *leu2*, *trp1*, *ura3*; suppressible marker *ade1-14*(UGA)] were prepared, co-transformed with sonicated Sup35NM amyloids and a URA3 marker plasmid and plated onto SD-Ura plates containing 1M sorbitol as described previously[8]. After 3-4 days of the protein infection, more than 100 randomly selected Ura$^+$ transformants on the SD-Ura plates (from different independent transformations) were patched onto modified YPD plates which enhance color phenotypes of [*PSI*$^+$] strains[8]. Transformation efficiencies and fractions of strong (white) and weak (pink) [*PSI*$^+$] strains were calculated by color on the YPD plates.

Crosslinking and isolation of Sup35NM oligomer. A single Sup35NM cysteine mutant at the C terminus (20μM) was reacted with sulfo-MBS (100μM) (Pierce) in 5mM potassium phosphate buffer containing 150mM sodium chloride (pH7.4) at 4°C according to the manufacturer's protocol and the reaction was stopped by the addition of 2-mercaptoethanol at a final concentration of 20mM. 500μL of the crosslinked sample was immediately applied to size exclusion chromatography (Superdex 200 HR column, GE) at a flow rate of 0.4ml/min, using 5mM potassium phosphate buffer

containing 150mM sodium chloride (pH7.4) and fractions of 1mL were collected. The same amount of each fraction (estimated by the absorbance at 280nm) was processed for western blotting with an anti-Sup35NM antibody and seeding experiments with Sup35NM monomers on a fluorescence plate reader.

Monitoring spontaneous and seeded amyloid formation with thioflavine T. Spontaneous and seeded amyloid formation were monitored with a plate reader (Spectra Max M2, Molecular device), using thioflavine T as a fluorescent probe[1]. Excitation of thioflavine T fluorescence was 442nm and emission was monitored at 485nm. Typical reactions include 2.5 μM Sup35NM and 20 μM thioflavine T in the 5mM potassium phosphate buffer containing 150mM sodium chloride (pH7.4) in the absence or presence of indicated seeds (10%). The lag time in spontaneous amyloid formation was determined by the time when fluorescence intensities reach 5% of the total intensities.

Figure legends of Supplementary Figures

Supplementary Figure 1

Disordered secondary structures of Sup35NM monomer at 4°C and 37°C and Sup35NM oligomer.

(**a**) Far-UV CD spectra of 5 μM Sup35NM monomer at 4°C (blue, solid line), 37°C (red, solid line), Sc4 amyloid (blue, broken line) and Sc37 amyloid (red, broken line).

(**b**) Far-UV CD spectra of 3 μM (black), 5 μM (red), 10 μM (green), and 15 μM (blue) Sup35NM measured at 4°C. The spectra were normalized to the molar elipticity at 220 nm for comparison of the spectral shapes clearly. Note, the similar spectral shape between 3μM Sup35NM and 15μM Sup35NM at 4°C indicates that the CD spectrum of Sup35NM oligomer is similar to that of Sup35NM monomer.

Supplementary Figure 2

Sup35NM oligomers are composed of 4-5 monomers.

AUC analysis for 10μM Sup35NM oligomers formed at 4°C. The number in each peak corresponds to that of Sup35NM monomer.

Supplementary Figure 3

Formation of wild-type Sup35NM amyloids in the presence of proline mutant seeds and their effects on prion strain phenotypes.

(**a,b**) Amyloid formation of 2.5μM wild-type Sup35NM in the presence of 10% seeds of the proline mutants that inhibit oligomer formation was monitored by thioflavine T fluorescence at 4°C (**a**) and 37°C. (**b**). (**c,d**) Amyloid formation of wild-type Sup35NM in the presence of seeds of the proline mutants that do not affect oligomer formation was monitored by thioflavine T fluorescence at 4°C (**c**) and 37°C (**d**). (**e**) Effects of wild-type Sup35NM amyloids seeded by the proline mutants on prion strain

phenotypes. Fractions of strong (white bar) and weak (pink bar) [*PSI*$^{+}$] phenotypes were determined. The fibers used for the amyloid infection were formed at 8°C.

Supplementary Figure 4

Nonnative interactions are critical for the formation of Sup35NM oligomer.

(**a,b**) Temperature dependence of pyrene excimer fluorescence intensity for the Cys88 (**a**) and Cys108 (**b**) mutants. Blue, cyan, green, yellow, orange, red and dotted black lines show spectra at 4, 6.5, 9, 12, 23, 37°C and 4°C (returned from 37°C), respectively.

Supplementary Figure 5

Sup35NM oligomer is not required for growth from preformed Sc4 seeds.

A fraction of strong and weak [*PSI*$^{+}$] phenotypes was evaluated by infecting [*psi*$^{-}$] yeast with Sc4 amyloid seeded by Sc4 or Sc37 fibers and Sc37 amyloid seeded by Sc37 fibers. Shown are fractions of strong (white bar) and weak (pink bar) [*PSI*$^{+}$] phenotypes as well as prion infectivity.

Supplementary Figure 6

Sup35NM oligomers and fibers show different reactivities to thioflavine T (ThT).

(**a**) Fluorescence intensities of ThT in the presence of Sup35NM in the amyloid (5μM) or soluble state at 4°C and 37°C. As fluorescence intensities change with temperature, fluorescence spectra were measured at both 4°C (blue) and 37°C (red). *Inset* shows a lower scale of fluorescence intensities of soluble Sup35NM for clarity.

(**b**) Sup35NM concentration-dependent increase in fluorescence intensities of ThT at 4°C.

(**c**) Temperature-dependent changes in fluorescence intensities of ThT for 0.45mg/mL Sup35NM (black) and BSA (white). ThT fluorescence intensities are plotted against temperature.

Supplementary Figure 7

Initially formed Sup35NM oligomers do not have seeding activities.

(**a**) An elution profile of Sup35NM oligomers and monomers by size exclusion chromatography. Values at the top show the molecular weight of protein markers and V denotes the void volume. (**b**) Western blot of the fractions 1-7 in (**a**) by an anti-Sup35NM antibody. Values on the left side show the molecular weight of protein markers. (**c**) Sup35NM amyloid formation in the presence of the fraction 1, 2 or 6 was monitored by thioflavine T fluorescence. Black, blue, red, green and grey lines show the amyloid formation of 2.5μM Sup35NM spontaneously or in the presence of the fraction 1, 2, 6 (14%) and wild-type amyloids (10%), respectively. (**d**) Normalized fluorescence intensities for the amyloid formation in (**c**).

Supplementary Figure 8

Spontaneous amyloid formation of Sup35NM proline and tryptophan mutants.

(**a,b**) Spontaneous amyloid formation of 2.5μM Sup35NM proline mutants was monitored by thioflavine T fluorescence at 4°C (**a**) and 37°C (**b**). (**c,d**) Spontaneous amyloid formation of 2.5μM Sup35NM tryptophan mutants was monitored by thioflavine T fluorescence at 4°C (**c**) and 37°C (**d**).

Supplementary Figure 9

The nucleus formed in the Sc37 amyloid formation is much smaller than Sup35NM oligomers formed at 4°C.

(**a,c**) Spontaneous amyloid formation of Sup35NM at 4°C (**a**) or 37°C (**b**) was monitored by thioflavine T fluorescence. Red, green, cyan, blue and black lines show profiles of amyloid formation at 1.33, 2.65, 5.30, 7.95, 10.6μM, respectively. (**c,d**) Normalized fluorescence intensities for spontaneous amyloid formation at 4°C (**c**) and

37°C (**d**) in (**a**) and (**b**), respectively. *Inset* shows a lower scale of fluorescence intensities at an initial phase of amyloid formation. The lag time in spontaneous amyloid formation was determined by the time when fluorescence intensities reach 5% of the total intensities (black line). (**e**) Dependence of lag time of spontaneous amyloid formation at 4°C (blue) and 37°C (red) on Sup35NM concentration.

Supplementary references

1. Collins, S. R., Douglass, A., Vale, R. D. & Weissman, J. S. Mechanism of prion propagation: amyloid growth occurs by monomer addition. *PLoS Biol*. **2**, e321 (2004).

2. Fujisawa, T. *et al*. Small-angle X-ray scattering station at the SPring-8 RIKEN beamline. *J. Appl. Crystallogr*. **33**, 797-800 (2000).

3. Tanaka, M. *et al*. Expansion of polyglutamine induces the formation of quasi-aggregate in the early stage of protein fibrillization. *J. Biol*. *Chem*. **278**, 34717-34724 (2003).

4. Ameyama, Y. *et al*. Large-aperture TV detector with a beryllium-windowed image intensifier for x-ray diffraction. *Rev. Sci. Instrum.* **66**, 2290-2294 (1995).

5. Ito, K., Kamikubo, H., Yagi, N. & Amemiya, Y. Correction method and software for image distortion and nonuniform response in charge-coupled device-based X-ray detectors utilizing X-ray image intensifier. *Jpn. Appl. Phys*. **44**, 8684-8691 (2005).

6. Guinier**,** A. & Fournet, G. Small-Angle Scattering of. X-rays. John Wiley & Sons, New York (1955).

7. Svergun, D. I., Semenyuk, A. V. & Feigin, L. A. Small-angle-scattering-data treatment by the regularization method, *Acta. Cryst.* **44**, 244-250 (1988).

8. Tanaka, M., Chien, P., Naber, N., Cooke, R. & Weissman, J. S. Conformational variations in an infectious protein determine prion strain differences. *Nature* **428**, 323-328 (2004).

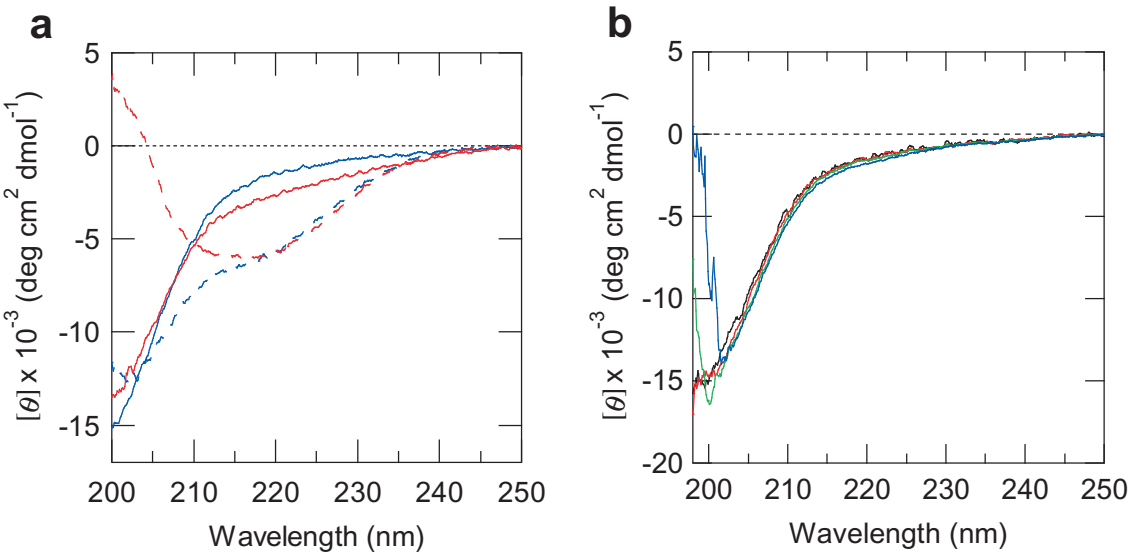

Ohhashi et al. Supplementary Fig. 1

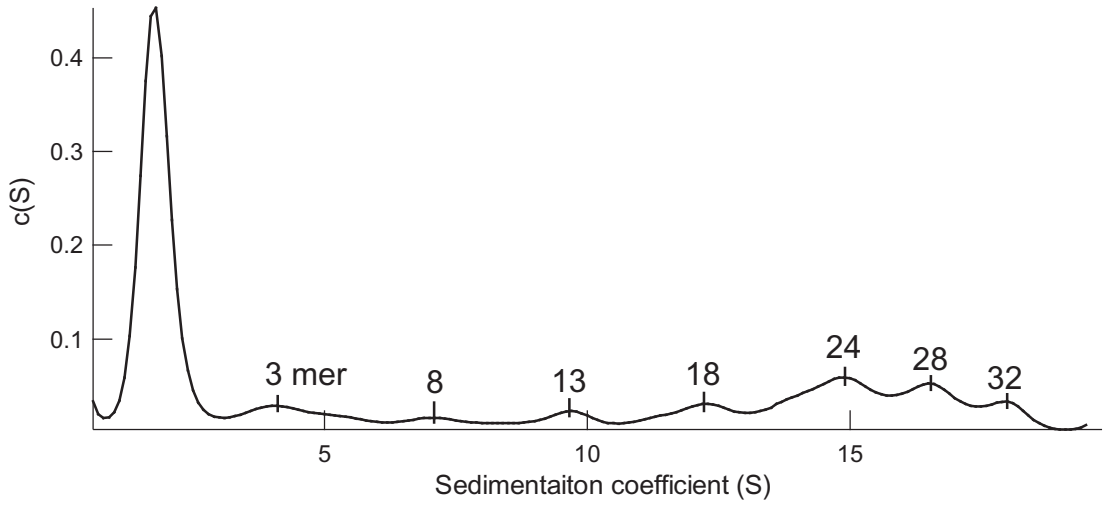

Ohhashi et al. Supplementary Fig. 2

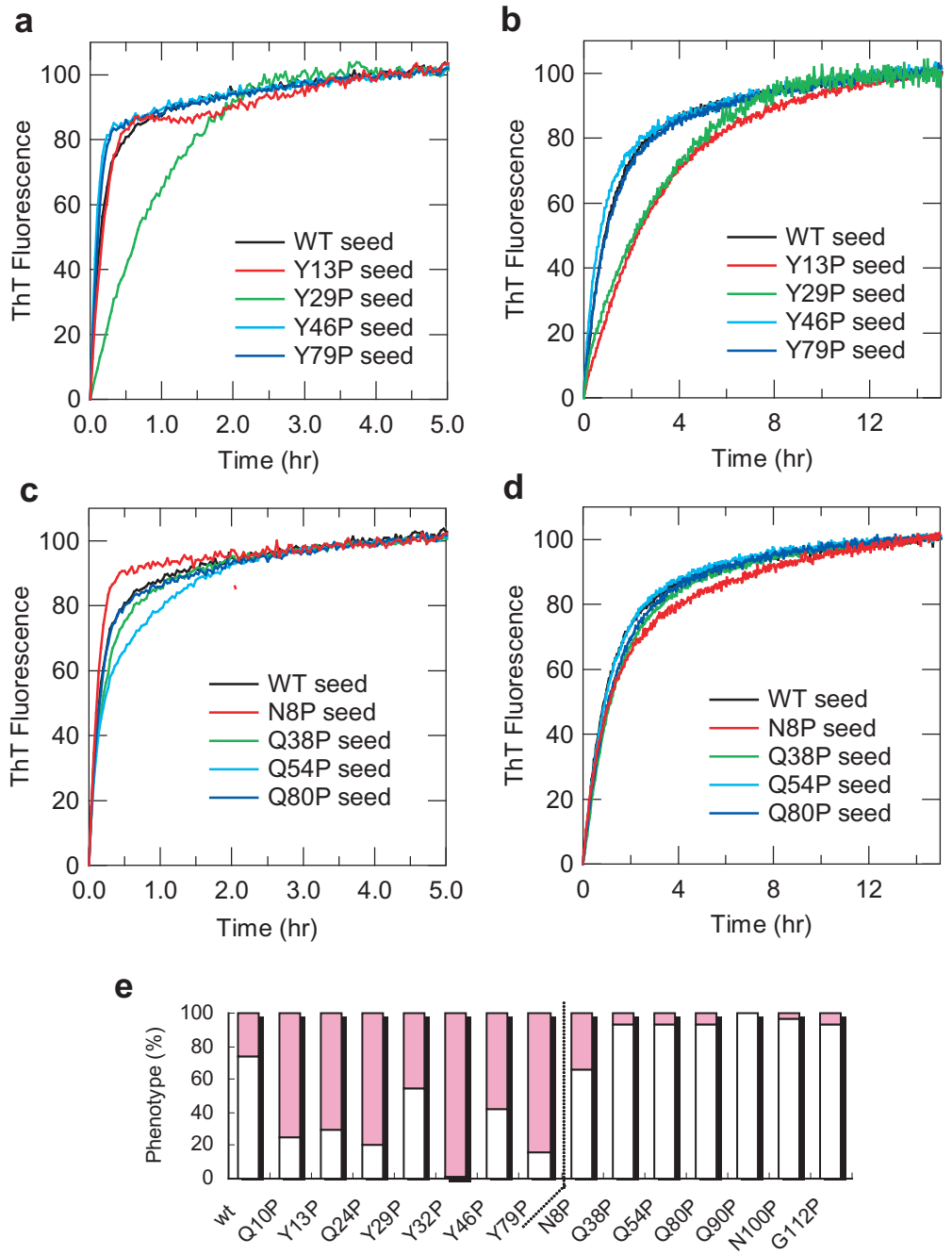

Ohhashi et al. Supplementary Fig. 3

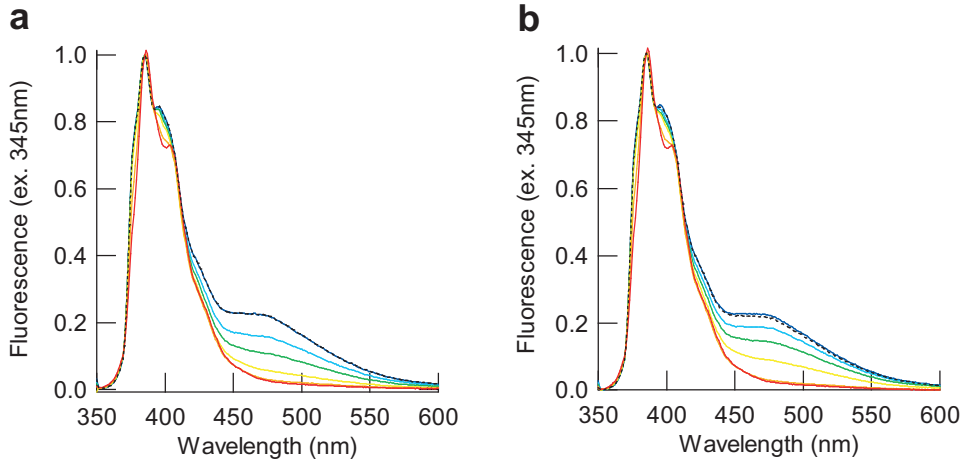

Ohhashi et al. Supplementary Fig. 4

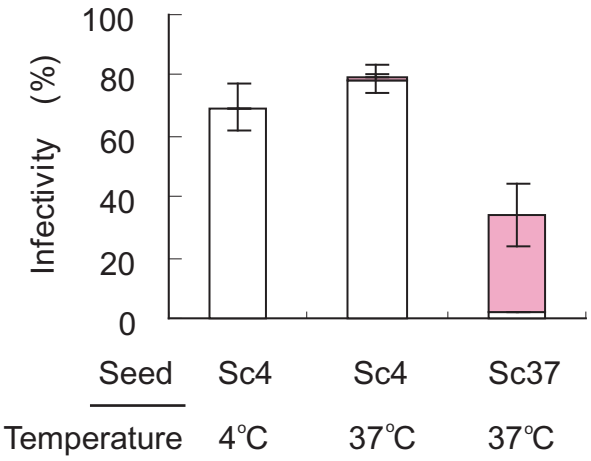

Ohhashi et al. Supplementary Fig. 5

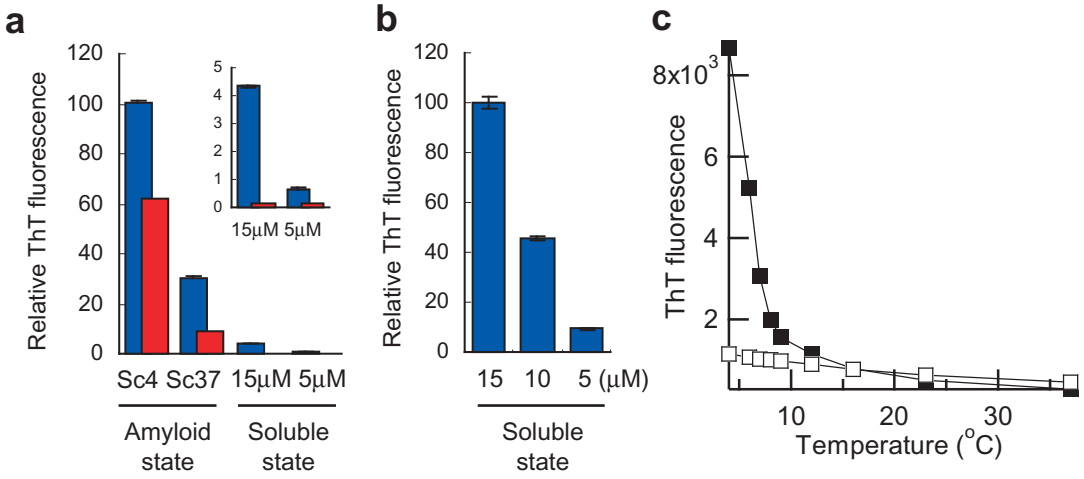

Ohhashi et al. Supplementary Fig. 6

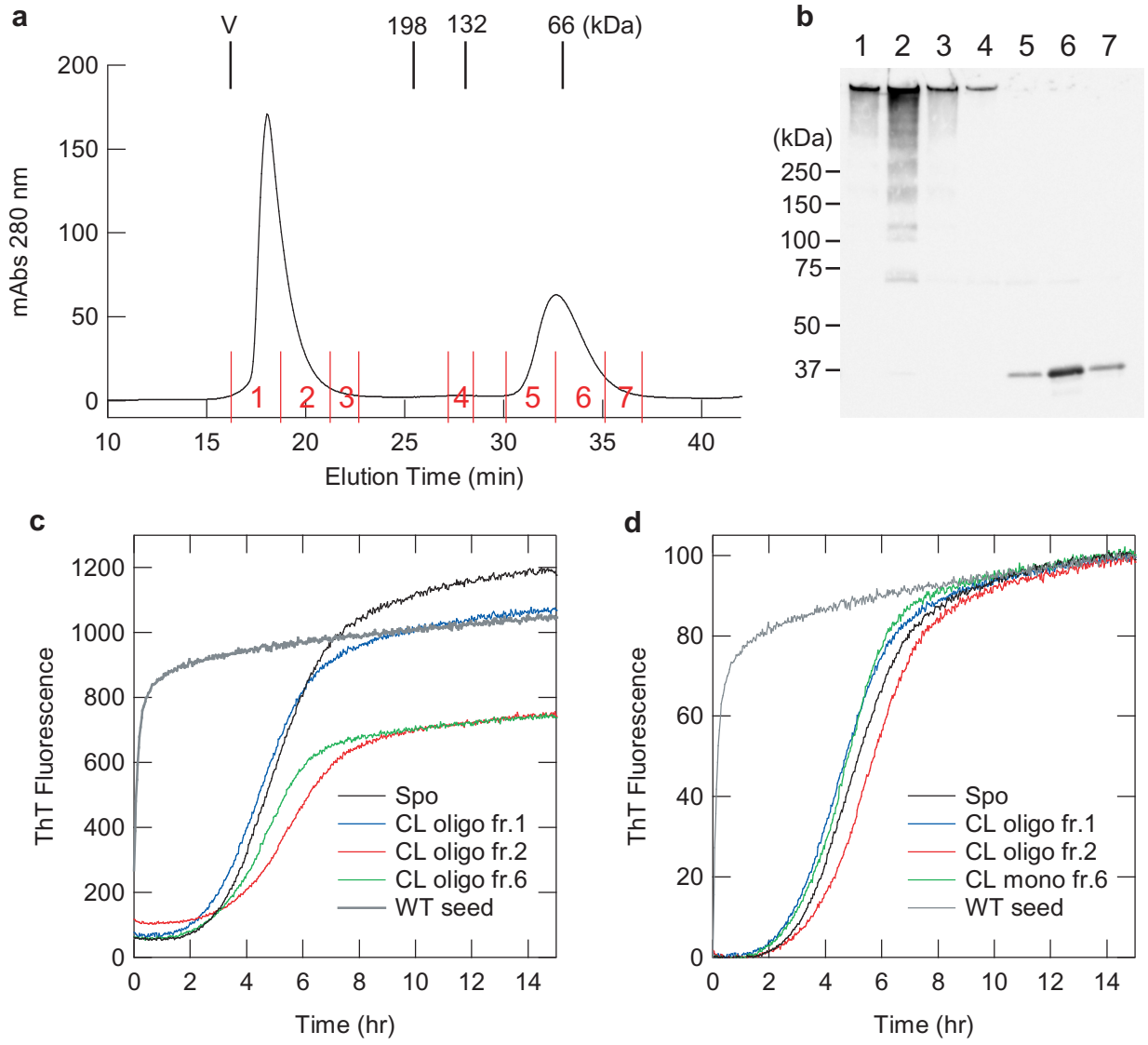

Ohhashi et al. Supplementary Fig. 7

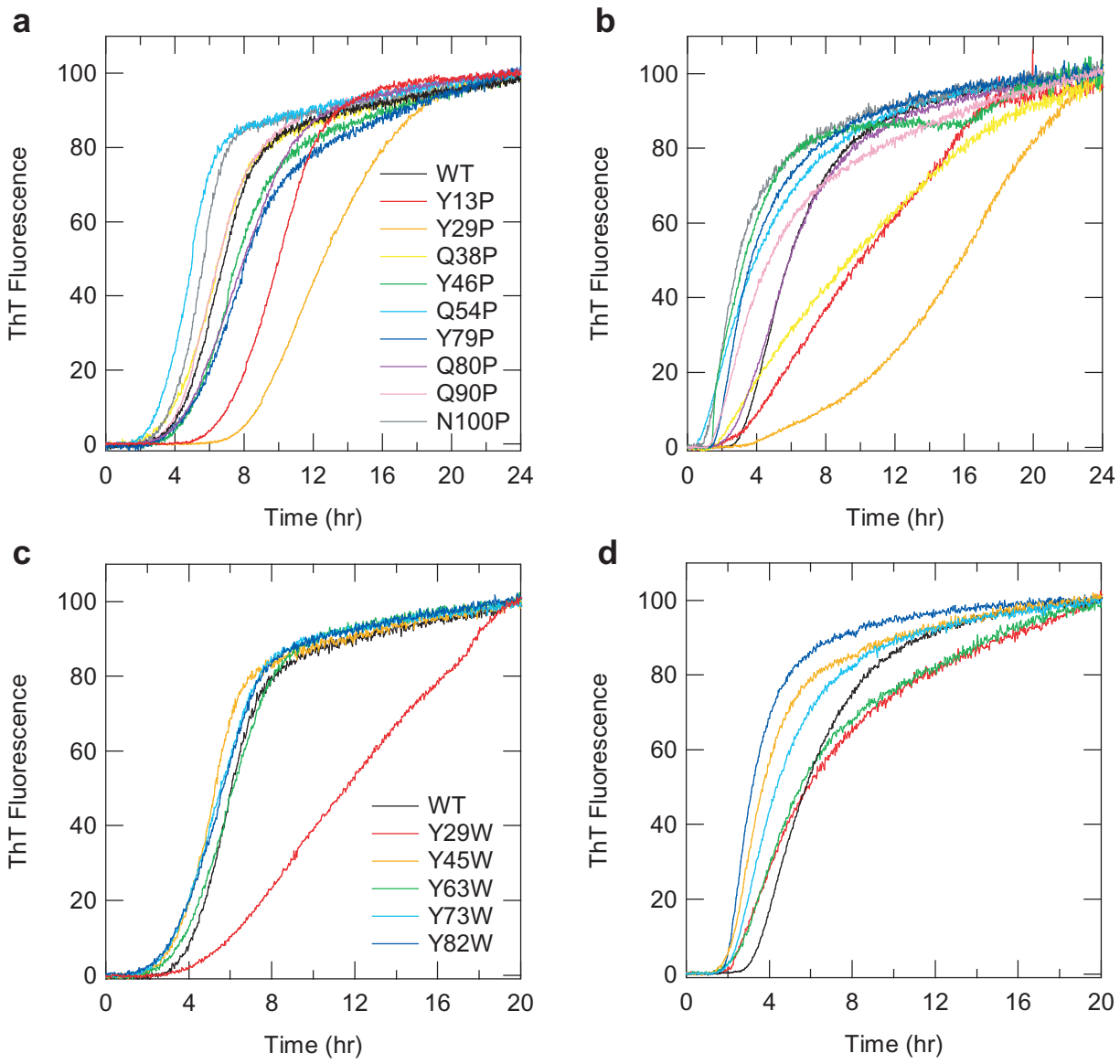

Ohhashi et al. Supplementary Fig. 8

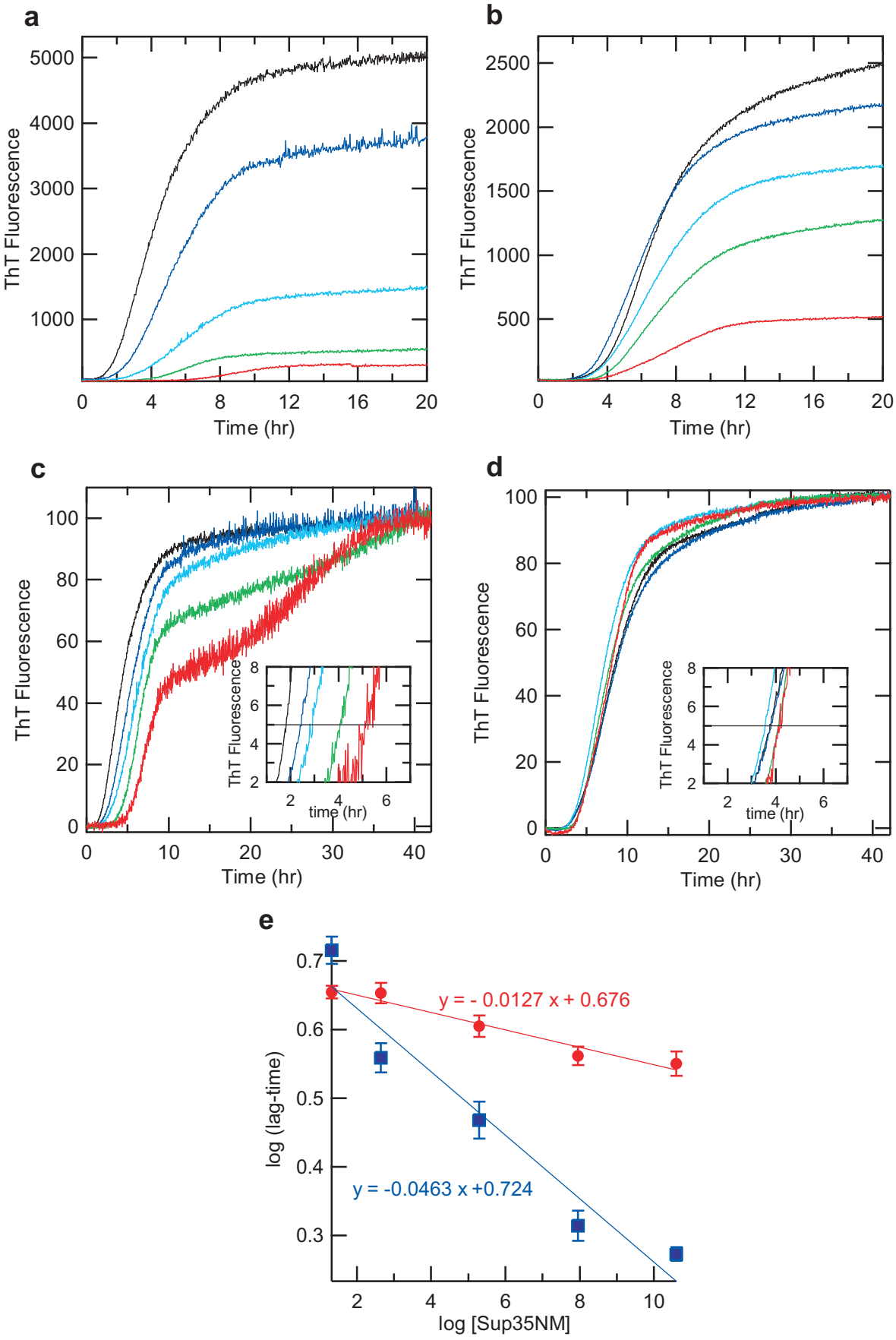

Ohhashi et al. Supplementary Fig. 9